JCI The Journal of Clinical Investigation

CD36 participates in a signaling pathway that regulates ROS formation in murine VSMCs

Wei Li, Maria Febbraio, Sekhar P. Reddy, Dae-Yeul Yu, Masayuki Yamamoto, Roy L. Silverstein

J Clin Invest. 2010;120(11):3996-4006. https://doi.org/10.1172/JCI42823.

Research Article **Cardiology**

CD36 is a membrane glycoprotein expressed on platelets, monocytes, macrophages, and several other cell types that was recently demonstrated to be involved in platelet activation in response to oxidized phospholipids, including oxidized LDL. Although the role of CD36 in other vascular cells has not been well defined, previous studies have demonstrated that cd36-knockout (*cd36*$^{-/-}$) mice have prolonged thrombosis times after vascular injury, which can be protective in the state of hyperlipidemia. Here, we found significantly less ROS in the vessel walls of *cd36*$^{-/-}$ mice compared with WT after chemically induced arterial injury, suggesting that CD36 may contribute to ROS generation in the VSMCs themselves. Gene expression analysis revealed that the antioxidant enzymes peroxiredoxin-2 (Prdx2) and heme oxygenase-1 were upregulated in *cd36*$^{-/-}$ VSMCs. Molecular dissection of the pathway in isolated mouse VSMCs revealed CD36 ligand-dependent induction of Fyn phosphorylation, with subsequent phosphorylation and degradation of the redox-sensitive transcription factor Nrf2. Chromatin immunoprecipitation experiments further showed that Nrf2 directly occupied the *Prdx2* promoter. The importance of this pathway was evidenced by increased ROS generation in *prdx2*$^{-/-}$ mice and decreased thrombosis times in both *prdx2*$^{-/-}$ and *nrf2*$^{-/-}$ mice after vascular injury. These data suggest that CD36-mediated downregulation of antioxidant systems in VSMCs may contribute to its prothrombotic, proinflammatory, and atherogenic effects.

CD36 participates in a signaling pathway that regulates ROS formation in murine VSMCs

Wei Li,[1,2] Maria Febbraio,[2,3] Sekhar P. Reddy,[4] Dae-Yeul Yu,[5] Masayuki Yamamoto,[6] and Roy L. Silverstein[1,2]

[1]Department of Cell Biology, Lerner Research Institute, Cleveland Clinic Foundation, [2]Department of Molecular Medicine, Cleveland Clinic Lerner College of Medicine, [3]Department of Molecular Cardiology, Lerner Research Institute, Cleveland Clinic Foundation, Cleveland, Ohio, USA. [4]Department of Environmental Health Sciences, Johns Hopkins Bloomberg School of Public Heath, Baltimore, Maryland, USA. [5]Aging Research Center, Korea Research Institute of Bioscience and Biotechnology, Daejeon, South Korea. [6]Department of Medical Biochemistry, Tohoku University Graduate School of Medicine, Sendai, Japan.

CD36 is a membrane glycoprotein expressed on platelets, monocytes, macrophages, and several other cell types that was recently demonstrated to be involved in platelet activation in response to oxidized phospholipids, including oxidized LDL. Although the role of CD36 in other vascular cells has not been well defined, previous studies have demonstrated that cd36-knockout (*cd36*$^{-/-}$) mice have prolonged thrombosis times after vascular injury, which can be protective in the state of hyperlipidemia. Here, we found significantly less ROS in the vessel walls of *cd36*$^{-/-}$ mice compared with WT after chemically induced arterial injury, suggesting that CD36 may contribute to ROS generation in the VSMCs themselves. Gene expression analysis revealed that the antioxidant enzymes peroxiredoxin-2 (Prdx2) and heme oxygenase-1 were upregulated in *cd36*$^{-/-}$ VSMCs. Molecular dissection of the pathway in isolated mouse VSMCs revealed CD36 ligand-dependent induction of Fyn phosphorylation, with subsequent phosphorylation and degradation of the redox-sensitive transcription factor Nrf2. Chromatin immunoprecipitation experiments further showed that Nrf2 directly occupied the *Prdx2* promoter. The importance of this pathway was evidenced by increased ROS generation in *prdx2*$^{-/-}$ mice and decreased thrombosis times in both *prdx2*$^{-/-}$ and *nrf2*$^{-/-}$ mice after vascular injury. These data suggest that CD36-mediated downregulation of antioxidant systems in VSMCs may contribute to its prothrombotic, proinflammatory, and atherogenic effects.

Introduction

CD36, a class B scavenger receptor, is an 88-kDa membrane glycoprotein expressed on platelets, monocytes, macrophages, and several other cell types (1). It is a multifunctional receptor with independent capacity to bind 3 major classes of ligands: modified phospholipids, long-chain fatty acids, and proteins containing thrombospondin structural homology domains. Although CD36 was first identified on platelets, its role in platelet function remained undefined until recently, when our group showed that CD36 promotes platelet activation in response to oxidized phospholipids, including oxidized LDL (oxLDL) (2). We found that genetic deletion of CD36 in mice protected them from the prothrombotic state associated with hyperlipidemia (2) and oxidant stress and also significantly prolonged thrombotic occlusion times after vascular injury induced by ferric chloride ($FeCl_3$) (3). The mechanisms underlying this phenotype remain incompletely understood, but the antithrombotic effects of CD36 deficiency were dependent on the dose of $FeCl_3$ used to induce injury (3) and platelet transfusion studies revealed that they were in part platelet dependent. Furthermore, CD36-mediated signaling through specific Src family kinases and MAPKs was shown to promote platelet activation after vascular injury (4). The endogenous CD36 ligands generated during $FeCl_3$-induced injury include endothelial cell–derived microparticles (EMPs), which we showed bind specifically to platelet CD36 and enhance platelet reactivity (3).

These studies, while showing a critical role for platelet CD36 in thrombosis, do not rule out a role for CD36-mediated signaling in other vascular cells in promoting thrombosis. Although CD36 is not expressed on large-vessel endothelial cells (5, 6), several groups have reported that VSMCs in culture express low levels of CD36 (7–12) and that expression can be upregulated by PPARγ (9). No function for CD36 has been identified, however, on VSMCs. Since $FeCl_3$ and other injuries induce thrombosis via generation of oxidant damage and since CD36 has been reported to promote ROS formation in macrophages in vitro and in a murine cerebral ischemia model in vivo (13, 14), we hypothesized that CD36 on VSMCs could contribute to vascular injury by generating further oxidant stress and that part of the "thrombo-protection" seen in *cd36*$^{-/-}$ mice is due to diminished ROS production in the vessel wall.

In this manuscript, we show that CD36 is abundantly expressed by murine arterial smooth muscle cells in vivo and in vitro and absence of CD36 attenuated ROS production in response to $FeCl_3$-induced vascular injury in a mouse carotid artery thrombosis model. Using proteomic and genetic approaches, we found that CD36 regulates expression of the antioxidant enzymes peroxiredoxin-2 (Prdx2) and heme oxygenase-1 (HO-1) in VSMCs, and defined a CD36-dependent pathway mediated by the redox-sensitive transcription factor, NF-E2–related factor-2 (Nrf2), responsible for this regulation. Targeting CD36 may enhance activity of Nrf2 and thereby provide an effective strategy to restore endogenous antioxidant defenses in cardiovascular diseases.

Conflict of interest: The authors have declared that no conflict of interest exists.
Citation for this article: *J Clin Invest.* 2010;120(11):3996–4006. doi:10.1172/JCI42823.

Results

Absence of CD36 attenuates ROS production and microparticle generation after arterial injury. To determine whether CD36 contributes to vascular oxidant stress after $FeCl_3$-induced carotid injury, we measured ROS formation in the vessel wall by direct injection of a fluorescent superoxide indicator, dihydroethidium (DHE), also known as hydroethidine, which forms 2-hydroethidium (EOH) after reacting with superoxide anion (15). In WT animals, we observed a rapid increase in vessel fluorescence that was dose and time dependent, peaking at approximately 7-fold that of baseline with 12.5% $FeCl_3$ (data not shown). Fluorescence intensity was significantly decreased in the vessel wall of *cd36*$^{-/-}$ mice compared with WT (Figure 1A). Laser confocal microscopy examination of cross sections of dissected thrombus-containing vessels demonstrated that the fluorescence was mainly within the vessel wall, not the cells within the thrombi (Figure 1B), suggesting that the origin of the ROS was vascular cells. The level of ROS in the vessel walls of *cd36*$^{-/-}$ mice was similar to that seen in WT mice treated with edaravone (3-methyl-1 phenyl-2-pyrazoline-5-1), a potent free radical scavenger (Figure 1C). Interestingly, edaravone administration significantly prolonged occlusion times in WT mice after $FeCl_3$-induced injury (Figure 1D), phenocopying untreated *cd36*$^{-/-}$ mice. Edaravone also induced a small but marked increase in the vessel occlusion time in *cd36*$^{-/-}$ mice injured with the high dose of $FeCl_3$ (not shown).

These data suggest that CD36-mediated enhancement of oxidant stress contributes to thrombosis. Since microparticles (MPs) can be generated from endothelial cells by oxidant stress and function as CD36-dependent platelet-activating ligands, we measured circulating MP levels after $FeCl_3$ injury by immunofluorescence microscopy and dot immunoblot assay. There was no difference in circulating endothelial-derived or total MP levels between WT and *cd36*$^{-/-}$ mice after sham operation (data not shown). Circulating levels of EMPs, however, increased in both WT and *cd36*$^{-/-}$ mice after carotid injury with 7.5% $FeCl_3$, but as seen in the dot blot assay (Figure 1E), levels were significantly lower in *cd36*$^{-/-}$ mice. Immunofluorescence analysis of the MPs showed fewer total MPs and EMPs in the *cd36*$^{-/-}$ mice. Injury with 12.5% $FeCl_3$ further increased circulating MPs, but no difference was seen between groups (data not shown). These results are consistent with our prior studies (3) showing decreased incorporation of endothelial antigens in clots induced in *cd36*$^{-/-}$ animals associated with protection from thrombosis after injury with 7.5% but not 12.5% $FeCl_3$.

Expression of Prdx2 is increased in the artery wall in cd36$^{-/-}$ *mice*. To determine potential mechanisms underlying the antioxidative effect of CD36 deletion in the vessel wall, we performed 2D difference gel electrophoresis comparing carotid artery segments from WT and *cd36*$^{-/-}$ mice. Proteins that were differentially expressed were then identified by mass spectrometry. One of the proteins with the greatest difference in expression (~2-fold) was the phase II antioxidant enzyme Prdx2, a member of a ubiquitous family of antioxidant enzymes known to detoxify ROS and reactive nitrogen oxide species (16, 17). To confirm differential Prdx2 expression, the contralateral noninjured carotid arteries from 18 experimental mice in which the left carotids were used for thrombosis assays were combined into 2 pools and analyzed by immunoblotting assay. As shown in Figure 2A, Prdx2 levels were 3- to 4-fold higher in the *cd36*$^{-/-}$ mice than in the WT. Expression levels of glutathione peroxidase-1, catalase, and superoxide dismutase-1 did not differ between *cd36*$^{-/-}$ and WT carotid arteries (not shown). Immunohistochemical stains of the thrombosed carotid artery segments revealed that Prdx2 was mainly localized in the smooth muscle layer and that the staining intensity was markedly higher in the *cd36*$^{-/-}$ mice (Figure 2B). Prdx2 expression was also examined in other cells and tissues, including bone marrow, macrophages, platelets, and heart. Levels were markedly higher in hearts from *cd36*$^{-/-}$ mice and modestly increased in bone marrow–derived cells (Figure 2, C–F), suggesting that CD36 may regulate Prdx2 levels in multiple cell types.

CD36 is expressed in thoracic aorta smooth muscle. Immunohistochemical staining demonstrated that CD36 is abundantly expressed in the aortae (Figure 3A) and carotid arteries (not shown) of WT C57BL/6 mice. To explore mechanisms by which CD36 influences Prdx2 expression in the vessel wall, VSMCs were cultured from explants of thoracic aortic arteries of *cd36*$^{-/-}$ and WT mice (18) These cells showed characteristic staining for smooth muscle actin by immunocytofluorescence microscopy (not shown), and RT-PCR assays confirmed *CD36* mRNA expression in WT but not in *cd36*$^{-/-}$ cells (Figure 3B). To demonstrate that the CD36 expressed by cultured VSMCs is functionally active, we showed that WT but not *cd36*$^{-/-}$ VSMCs bound and internalized 1,1′-dioctadecyl-3,3,3′,3′-tetramethylindocarbocyanine perchlorate–labeled (DiI-labeled) NO_2LDL, a form of oxLDL that is a highly specific CD36 ligand (not shown).

Nrf2 regulates transcription of the Prdx2 gene promoter. A cis-acting antioxidant responsive element (ARE) regulates transcription of many genes encoding detoxification enzymes and antioxidant proteins that function in cellular defense systems (19). The transcription factor Nrf2 is the major regulator of ARE-driven gene expression, but whether Nrf2 regulates Prdx2 transcription is not known. By analyzing the nucleotide sequences 10 kb upstream of the Prdx2 ATG translational start site, we identified a core ARE (cARE) site (TGACTCTGCA) at position –8518 to –8508, a so-called extended ARE (eARE) site (TGAGGTAGCA) at –7836 to –7826, and 2 "eARE-like" sites located between the core and extended sites (20), suggesting that Nrf2 may regulate Prdx2 expression (Supplemental Figure 1; supplemental material available online with this article; doi:10.1172/JCI42823DS1). We therefore performed ChIP assays to determine whether Nrf2 binds to the putative ARE sites in the Prdx2 promoter using the cultured VSMCs. As shown in Figure 4A, an antibody to Nrf2 precipitated the cARE and eARE sites from both WT and *cd36*$^{-/-}$ VSMCs, suggesting that Nrf2 may regulate Prdx2 expression. To determine whether Nrf2 binding to the Prdx2 promoter sites has functional consequences, an 869-bp region from the Prdx2 promoter that includes the cARE, eARE, and eARE-like sites (P6; Figure 4B), as well as truncated constructs (P1–P5: Figure 4B), was cloned into a luciferase reporter vector, pGL2-Basic, and transfected into WT VSMCs using Lipofectamine LTX and Plus Reagent. Luciferase reporter activities examined 48 hours later showed (Figure 4C) that constructs containing the eARE site but not the cARE site induced significant luciferase activity, indicating that the eARE alone is sufficient to induce transcription. Luciferase activity was increased by another 2-fold with P6, indicating that the cARE site may contribute to transcriptional activity, but the absence of luciferase activity with P1 suggests that cARE alone is not sufficient to induce transcription. The "eARE-like" sites had no activity, either alone (P2) or on combination with eARE (P5 vs. P3) or with cARE (P4 vs. P1). Mutations in the eARE site (Figure 4B) at sequences previously shown to inhibit activity in other systems (21) significantly diminished luciferase reporter activity (M1, M2, and M3; Figure 4C), further demonstrating that a functional eARE site plays a key role in Nrf2-mediated Prdx2 expression.

We next sought to determine whether Nrf2 could induce Prdx2 expression in vascular cells. A plasmid expression vector encoding mouse Nrf2 was used to generate a pool of Nrf2-overexpress-

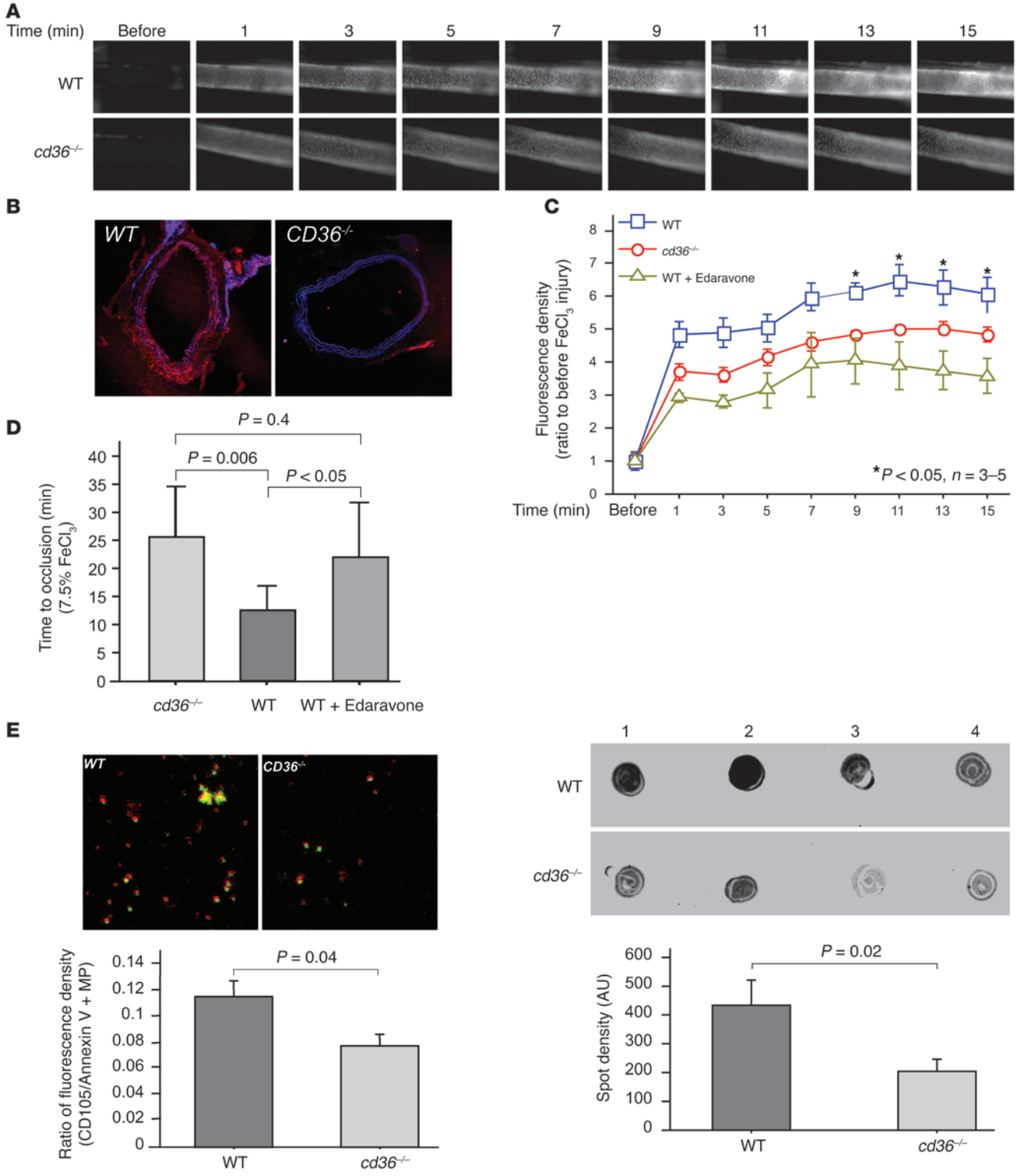
A
Time (min)
Before
1
3
5
7
9
11
13
15
WT
cd36−/−
B
WT
CD36−/−
C
WT
cd36−/−
WT + Edaravone
Fluorescence density (ratio to before FeCl3 injury)
*P < 0.05, n = 3–5
Time (min)
Before
D
P = 0.4
P = 0.006
P < 0.05
Time to occlusion (min) (7.5% FeCl3)
cd36−/−
WT
WT + Edaravone
E
WT
CD36−/−
P = 0.04
Ratio of fluorescence density (CD105/Annexin V + MP)
WT
cd36−/−
1
2
3
4
WT
cd36−/−
P = 0.02
Spot density (AU)
WT
cd36−/−

Figure 1
CD36 deficiency decreased ROS formation in the vessel wall in response to chemical injury and reduced endothelial microparticle generation. (**A**) ROS formation is diminished in the vessel wall of *cd36*$^{-/-}$ mice. Hydroethidine (10 μg/g in 150 μl saline) was injected into the jugular veins, and the carotid arteries were imaged using intravital microscopy before and after $FeCl_3$ treatment. (**B**) ROS formation after $FeCl_3$ injury is located within the vessel wall. Cross sections of the above vessels were examined with laser confocal microscopy. Blue represents autofluorescence of elastic lamina. Red is from 2-hydroxyethidium/ethidium and reflects ROS formed after $FeCl_3$ treatment. Original magnification, ×400. (**C**) Edaravone, a free radical scavenger, decreases ROS formation to an extent similar to that seen in *cd36*$^{-/-}$ mice. Edaravone (1 mg/kg) and hydroethidine were directly injected into the jugular veins of the WT mice, and ROS formation on the vessel wall was examined as in **A**. The fluorescence density of each frame was analyzed by NIH image. (**D**) Inhibition of ROS formation prolongs occlusion time after $FeCl_3$ injury. Edaravone was injected into the jugular veins as above, and time to form an occlusive thrombus was measured after carotid artery injury by $FeCl_3$. One-way ANOVA (Bonferroni/Dunn) was used to determine the differences among groups (**A** and **D**). (**E**) EMPs are decreased in plasma from *cd36*$^{-/-}$ mice after $FeCl_3$ injury. Mice were injected with heparin sulfate (100 USP), and then the carotid arteries were injured with $FeCl_3$. 5 minutes later, whole blood was harvested by heart puncture and MPs were collected by centrifugation. EMPs were evaluated by laser confocal microscopy (left panels) using antibodies to CD105 (green) and annexin V (red) and by dot immunoblot (right panels) using anti-CD105. Original magnification, ×5040. Data are represented as mean ± SEM.

ing mouse VSMCs, and immunoblots of lysates from these cells demonstrated dramatic upregulation of Prdx2 expression compared with that of cells transfected with a control plasmid, empty pCDNA3 (Figure 4D).

CD36 inhibits Nrf2 nuclear localization in VSMCs. Nrf2 is normally sequestered in the cytoplasm by a binding partner, Keap1, but activation signals including electrophiles and oxidant stress disrupt the Nrf2/Keap1 complex, allowing Nrf2 to translocate to the nucleus where it binds ARE sequences and induces transcription of specific genes. To determine whether CD36 signaling regulates Nrf2 and subsequently Prdx2 expression in the vessel wall, we first demonstrated by real-time PCR that *prdx2* mRNA levels were significantly higher in *cd36*$^{-/-}$ VSMCs than in WT cells (Figure 5A). Immunoblot assays showed that Prdx2 and Nrf2 protein expression were also significantly higher in *cd36*$^{-/-}$ VSMCs compared with WT (Figure 5B). Importantly, cellular fractionation studies showed that Nrf2 accumulated in the nuclei of *cd36*$^{-/-}$ cells to a far greater extent than in WT cells (Figure 5C). Cytosolic Nrf2 levels were also slightly higher in *cd36*$^{-/-}$ VSMCs (Figure 5D). In these experiments, the efficacy of cell fractionation was documented using anti-TATA binding protein and anti–α-tubulin antibodies to detect nuclear and cytoplasmic proteins, respectively. To further demonstrate that deletion of *cd36* induced Prdx2 overexpression via Nrf2 signaling, Nrf2 expression was knocked down in *cd36*$^{-/-}$ VSMCs using shRNA, and Prdx2 expression was shown to be significantly decreased (Figure 5E). These data suggest that CD36-mediated signaling may inhibit Nrf2 nuclear translocation and/or promote Nrf2 nuclear export and degradation.

Fyn plays a key role in controlling Nrf2 nuclear translocation. A common theme in CD36 signal transduction in platelets, mononuclear phagocytes, and endothelial cells is activation of specific Src family kinases, including Fyn and Lyn (1, 22). Studies by Jain and Jaiswal in hepatoma cells demonstrated that Fyn-induced phosphorylation of Nrf2 at tyrosine 568 led to nuclear export and degradation (23). We thus hypothesized that CD36-dependent activation of Fyn in VSMCs would lead to Nrf2 degradation and hence decreased Prdx2 expression. To explore this hypothesis, we first examined whether inhibition of Src family kinase activity affected Nrf2 nuclear accumulation in VSMCs. As shown by immunofluorescence in Figure 6A (PP2), a broadly active Src family kinase inhibitor significantly increased nuclear Nrf2 in WT VSMCs, but caused less of an increase in *cd36*$^{-/-}$ cells, suggesting that Src kinases may play some role in Nrf2 nuclear export or degradation. The fact that cells treated with PP3, a nonactive control analog of PP2, showed significantly lower nuclear Nrf2 in WT VSMCs than in *cd36*$^{-/-}$ cells is consistent with the Western blot assay of nuclear/cytosol fractionation showed in Figure 5C. Treatment of WT VSMCs with 1-(Palmitoyl)-2-(5-keto-6-octene-dioyl)phosphatidylcholine (KodiA-PC) (24), a specific CD36 ligand, dramatically increased Fyn phosphorylation (Figure 6B), suggesting functional CD36/Fyn signaling in VSMCs. Interestingly, tyrosine-phosphorylated Nrf2 also increased in the same manner (Figure 6B). These data strongly suggest that CD36 controls Nrf2 activity by regulating Fyn activity. In further support of this conclusion, we found that VSMCs cultured from thoracic aortae of *fyn*$^{-/-}$ mice markedly increased Nrf2 and Prdx2 expression compared with WT cells (Figure 6C).

CD36 inhibits response to oxidative stress in vitro, and expression of Prdx2 and Nrf2 in the vessel wall contributes to antithrombotic effects in vivo. To determine whether the increase in Nrf2 activity associated with deletion of CD36 protects vascular cells from oxidative stress, VSMCs were serum starved for 24 hours and then reexposed to 10% serum in the presence or absence of 250 μM H_2O_2 for timed periods up to 6 hours. Figure 7A shows that H_2O_2 induced dramatically more HO-1 expression in *cd36*$^{-/-}$ cells compared with WT, with induction seen as early as 3 hours and increasing further at 6 hours. Lower (50 μM) or higher (1 mM) concentrations of H_2O_2 produced similar effects (not shown). These data suggest that CD36 expression inhibits the antioxidant system in response to oxidant stimulation.

To further demonstrate the prooxidant effect of CD36, VSMCs were treated with different concentration of $FeCl_3$ and cellular ROS generation was quantified by HPLC detection of EOH (25, 26). $FeCl_3$ increased superoxide generation in a dose-dependent manner, as has been previously reported (27). The level of EOH was significantly lower in $FeCl_3$-treated *cd36*$^{-/-}$ cells compared with WT VSMCs and was no different in treated *cd36*$^{-/-}$ cells than untreated cells (Figure 7B). To show whether Prdx2 overexpression in WT VSMCs phenocopies *cd36*$^{-/-}$ cells, human Prdx2 cDNA was transfected into WT VSMCs and a cell pool was generated by G418 selection. Prdx2 overexpression significantly decreased $FeCl_3$-induced superoxide anion generation when compared with WT VSMCs, almost to the level seen in *cd36*$^{-/-}$ (Figure 7B). In contrast, shRNA-based gene knockdown of *nrf2* in *cd36*$^{-/-}$ cells significantly increased $FeCl_3$-induced superoxide formation when compared with *cd36*$^{-/-}$ cells. These data show that both loss of *cd36* and overexpression of Prdx2 provoke a strong oxidant effect and *cd36*$^{-/-}$ induced antioxidant effect via upregulation of Nrf2 and Prdx2.

To show that Prdx2 expression in the vessel wall may induce a protective effect in vivo, we measured ROS generation after $FeCl_3$-induced carotid injury in *prdx2*$^{-/-}$ mice. As predicted, $FeCl_3$ treatment induced more ROS generation in the vessel walls of *prdx2*$^{-/-}$ mice than in *prdx2* WT mice (Figure 7C). Importantly, arterial thrombi formed more quickly and were larger in both *prdx2*- and *nrf2*$^{-/-}$ mice compared with WT, resulting in a significantly shorter time to occlusion (Figure 7D).

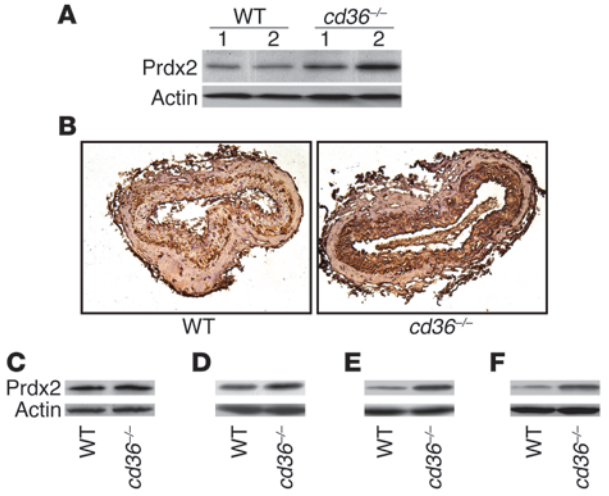

Figure 2
CD36 deficiency is associated with increased Prdx2 expression in the vessel wall. (**A**) Western blot assay of Prdx2 expression was performed using tissue lysates prepared from carotid arteries. 9 vessels were pooled in each group (n = 2). Actin was used as loading control. (**B**) Anti-Prdx2 immunohistochemical staining of cross sections from thrombosed carotid arteries comparing vessels from WT animals (left) with those from *cd36*$^{-/-}$ animals (right). (**C**–**F**) Western blotting assays of Prdx2 expression in other tissues and cells obtained from C57BL/6 mice. (**C**) Bone marrow cells; (**D**) macrophages; (**E**) platelets; (**F**) hearts. Actin was used as a loading control.

Discussion

Obstructive and thrombotic cardiovascular diseases are multifactorial and involve complex interplay among lifestyle (diet, smoking, exercise, ethanol consumption) and fixed (genotype, age, menopausal status, sex) causative factors (28). An initiating step is often endothelial injury induced by cellular oxidative stress precipitated by the production of damaging ROS by many cell types including VSMCs and monocytes/macrophages (28). Endothelial injury can promote thrombosis by multiple mechanisms, including generation of MPs. ROS also contribute to injury by oxidizing lipoproteins such as LDL within the vessel wall, facilitating uptake of these particles by macrophages. Under conditions in which lipid uptake cannot be balanced by natural efflux pathways, lipids accumulate in the cells, leading to formation of foam cells, a hallmark of early atherosclerotic lesions (1, 29, 30). Foam cells are also a source of inflammatory cytokines and further ROS production, contributing to lesion progression. CD36 plays several important roles in these processes (31–33). On macrophages and platelets, it is a critical receptor for oxLDL and MPs (1, 3) and its engagement by these ligands activates the cells, contributing to the thromboinflammatory state (1, 3, 4, 34). CD36-mediated oxLDL uptake by macrophages is essential for foam cell formation in vitro and in vivo and CD36 signaling in macrophages alters cytoskeletal dynamics, inhibiting migration and thus preventing egress of the cells from atheroinflammatory lesions (35).

To this point, evidence linking CD36 to human atherothrombotic disease includes reports that CD36 genetic polymorphisms are associated with myocardial infarction (36, 37) and that hyperlipidemia is associated with CD36-dependent platelet hyperreactivity (2). Numerous studies of mouse model systems have validated the importance of CD36 in vascular disease. *cd36*$^{-/-}$ mice show diminished atherosclerosis in both *apoe*- and *ldlr*$^{-/-}$ backgrounds (33, 38), demonstrate decreased ischemia/reperfusion injury after cerebral infarction (13), and are partially protected from pathological thrombosis in response to vascular injury (3). In this manuscript, we demonstrate what we believe is a novel mechanism by which CD36 participates in the vascular injury response and also for the first time, to our knowledge, demonstrate a biological function for CD36 on vascular smooth muscle cells. We found that CD36 mediates VSMC ROS generation in vitro and in vivo by downregulating expression of the redox-sensitive transcription factor Nrf2, which in turn leads to loss of expression of phase II antioxidant enzymes, including Prdx2 and HO-1.

Figure 8 outlines a model for this CD36-regulated pathway. Oxidative vascular injury, such as that induced by hyperlipidemia and inflammation in *apoe*$^{-/-}$ mouse atherosclerosis models or by topical $FeCl_3$ application in commonly used murine thrombosis models, leads to dissociation of the transcription factor Nrf2 from its cytoplasmic partner, Keap1/INrf2. Nrf2 then enters the nucleus, where it binds to specific ARE elements in key antioxidant genes, including *HO-1* and *prdx2*. Expression of these genes then attenuates oxidant stress. Oxidative stress, however, also leads to generation of specific CD36 ligands, such as MPs and oxidized phospholipids. Engagement of these ligands by CD36 recruits and activates Fyn kinase, which in turn phosphorylates Nrf2. Phosphorylated Nrf2 is transported out of the nucleus and degraded. CD36 in VSMCs thus sensitizes the cells to oxidant stress, contributing to atherogenesis and thrombosis. Our observation that *prdx2*$^{-/-}$ mice as well as *nrf2*$^{-/-}$ mice showed a prothrombotic phenotype after $FeCl_3$-induced injury highlights the importance of this endogenous antioxidant system in vivo. Interestingly, we observed increased expression of Nrf2 and Prdx2 in VSMCs from *fyn*$^{-/-}$ mice, phenocopying the *cd36* nulls and strongly supporting the model that CD36-mediated Fyn activation is a critical component of the pathway. The data presented in this paper also show enhanced expression of the antioxidant pathway in *cd36*$^{-/-}$ mice under basal conditions. This raises the possibility that some CD36-mediated effects are ligand independent, although we cannot rule out the presence of endogenous CD36 ligands in these studies.

Attenuation of endogenous antioxidant systems is probably not the sole mechanism by which CD36 promotes ROS generation. Studies from our lab and others strongly suggest that CD36 signaling in macrophages directly induces ROS formation; blockade of CD36 or inhibition of NADPH oxidase (Nox) decreased oxLDL-induced ROS formation (35, 39). The intracellular pathway from

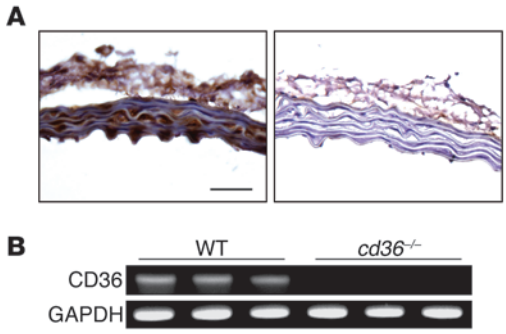

Figure 3
CD36 is expressed by arterial vascular smooth muscle cells. (**A**) Anti-CD36 immunohistochemical staining of cross sections from WT aortic artery (left panel). Nonimmune rabbit IgG was used as negative control (right panel). Scale bar: 40 μm. (**B**) RT-PCR assay of *CD36* mRNA expression in cultured VSMCs.

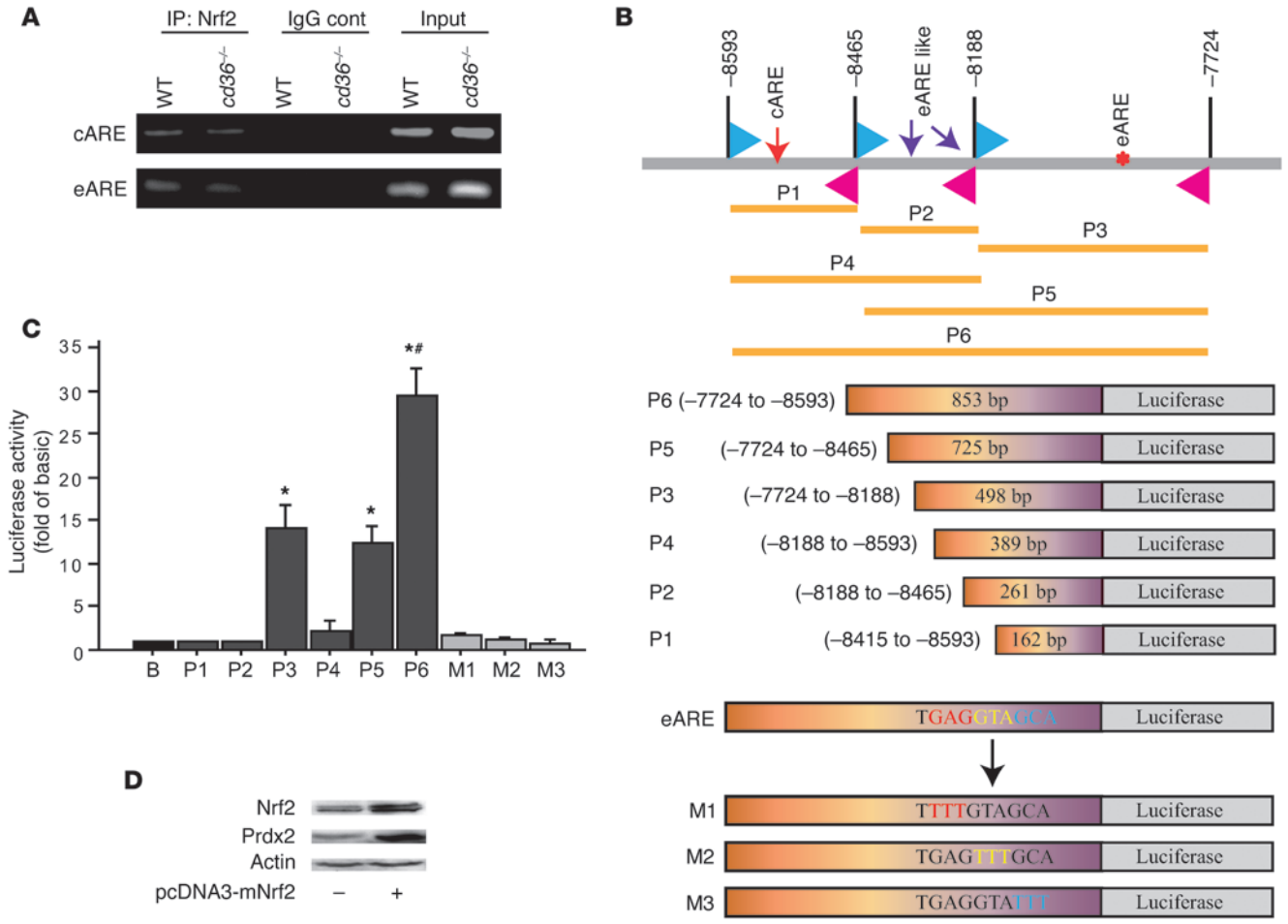

Figure 4

The transcription factor Nrf2 regulates Prdx2 expression. (**A**) ChIP assays. Both cARE and eARE sites were amplified from input of WT and *cd36*$^{-/-}$ VSMCs using specific primers as indicated in Methods. An antibody to Nrf2 precipitated the cARE and eARE sites from both WT and *cd36*$^{-/-}$ VSMCs. Nonimmune IgG control antibody did not precipitate these sites. (**B**) Schema of the Prdx2 promoter regions examined by luciferase expression assay. An 869-bp region from the Prdx2 promoter that includes the cARE, eARE, and eARE-like sites (P6) as well as truncated constructs containing only the cARE (P1) or eARE (P3) sites, the cARE or eARE with the eARE-like sites (P4 and P5), or the eARE-like sites without cARE or eARE sites (P2) were cloned into a luciferase reporter vector, pGL2-Basic. 3 additional constructs (M1–M3) were generated in which sets of 3 adjacent nucleotide triplets within the eARE site were mutated to TTT. (**C**) Luciferase reporter activity of Prdx2 promoter sequence. Plasmid vectors containing the Prdx2 promoter sequences were transfected into the WT VSMCs and luciferase activity examined 48 hours later. The luciferase signals were adjusted by protein concentration and expressed as fold change compared with basal levels. *$P < 0.0001$ vs. B, P1, P2, P4, and M1–M3; #$P < 0.001$ P6 vs. P3 and P5. (**D**) Nrf2 cDNA transfection induces Prdx2 expression in VSMCs. Plasmid vector pcDNA3 encoding mouse Nrf2 cDNA (pcDNA3-mNrf2) or empty vector was transfected into WT VSMCs, and expression of Nrf2 and Prdx2 were quantified by Western blot. One-way ANOVA (Bonferroni/Dunn) was used to determine the differences among groups. Data are represented as mean ± SEM.

CD36 to Nox has not been delineated, but recent studies from our lab and others show that CD36 may activate Vav family guanine nucleotide exchange factors. These are known to influence activation of the small molecular weight G proteins associated with Nox.

Interestingly, several studies have reported that Nrf2 regulates CD36 expression in macrophages and preadipocytes in response to oxLDL stimulation (40–43), suggesting that oxidative stress might "feed forward" through CD36 to decrease natural antioxidant responses and promote further injury. A recent paper by Sussan et al., however, surprisingly showed that loss of Nrf2 was protective against development of atherosclerosis (44), perhaps related to decrease in macrophage CD36 expression. This observation is discordant with many reports supporting the hypothesis that prooxidant conditions promote atherosclerosis while antioxidant conditions protect. Indeed, a different group clearly demonstrated that macrophage Nrf2 expression did not promote atherosclerosis in hyperlipidemic *ldlr*$^{-/-}$ mice and that Nrf2 was atheroprotective in early stages of atherogenesis (45). Together, these data suggest that the cellular context of Nrf2 expression, its downstream activities, and the regulation of its activity are complex and that further studies are necessary to reveal the mechanistic connections among Nrf2, CD36, and vascular disease.

In summary, we have shown that deletion of CD36-attenuated ROS production in response to $FeCl_3$ induced vascular injury in a mouse carotid artery thrombosis model and defined a CD36-dependent signaling pathway in VSMCs mediated by the redox-

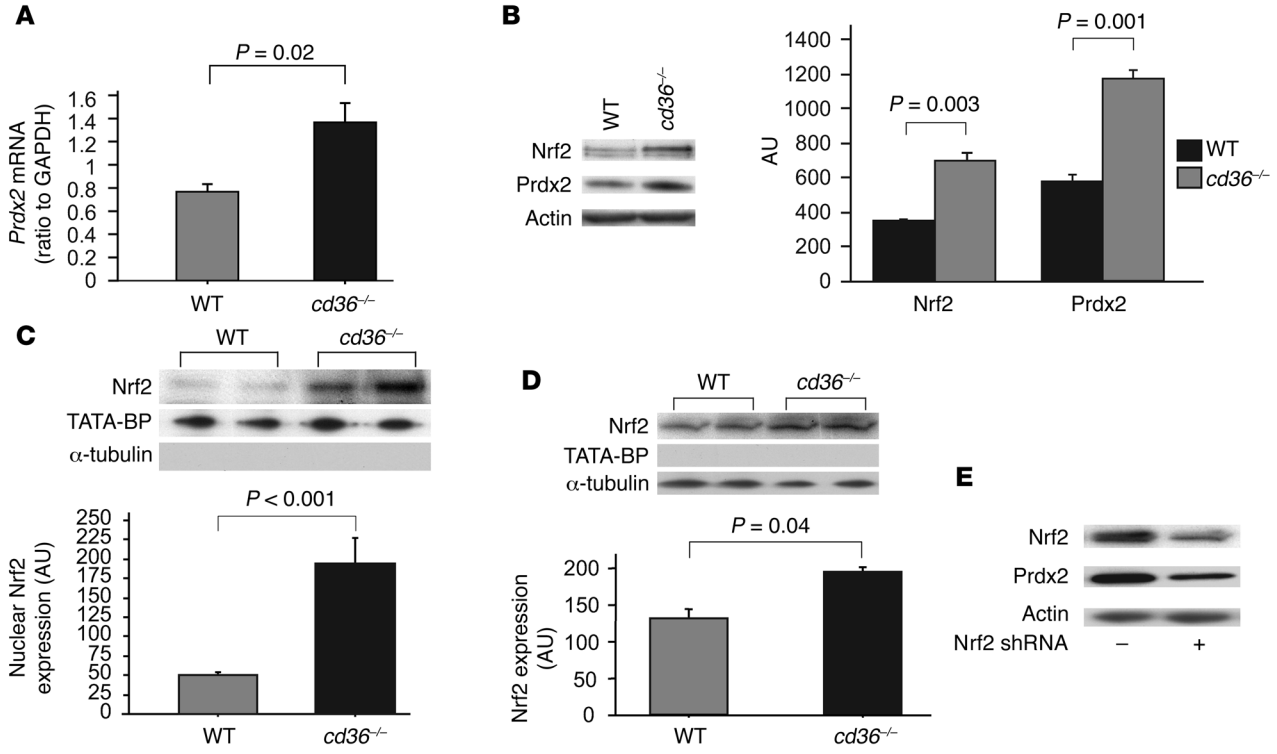

Figure 5

CD36 inhibits Nrf2 nuclear translocation. (**A**) Real-time PCR–based *Prdx2* mRNA quantitation. VSMCs were seeded at 10^6/10 cm plate, cultured overnight, and synchronized for 24 hours. The cells were then restimulated with serum (10%) in culture media for 3 hours and total RNA was extracted for real-time PCR assay. Data are shown as the ratio of Prdx2 to GAPDH. (**B**) Nrf2 and Prdx2 expression are increased in *cd36*$^{-/-}$ VSMCs. Confluent VSMCs from WT and *cd36*$^{-/-}$ cells were lysed and examined by Western blot for Nrf2 and Prdx2 expression. (**C** and **D**) *cd36*$^{-/-}$ cells show increased Nrf2 nuclear localization. Nuclear (**C**) and cytosolic (**D**) fractions were extracted from cultured cells and immunoblots performed with anti-Nrf2 antibody. TATA binding protein (TATA-BP) and α-tubulin were used to confirm the efficacy of cytosol and nuclear fractionation and as loading controls. Bar graphs in **B**–**D** show cumulative data of Western blot band densities that were analyzed by ATTO densitometry; $n = 3$–4. (**E**) shRNA-mediated knockdown of Nrf2 in *cd36*$^{-/-}$ cells decreases Prdx2 expression. A plasmid vector encoding shRNA that targets mouse Nrf2 was transfected into *cd36*$^{-/-}$ VSMCs, and a cell pool was generated with puromycin selection. Nrf2 and Prdx2 expression were examined by Western blot. Actin was reblotted as loading control. Data are represented as mean ± SEM.

sensitive transcription factor Nrf2, which downregulates endogenous antioxidant defenses. Transfection of Nrf2 or its downstream targets (such as HO-1) has been shown to inhibit ROS generation in vitro and in vivo and to ameliorate atherosclerosis and obstructive vascular diseases (46–48). These results are consistent with our model and suggest that targeting CD36 could enhance the Nrf2 pathway and provide a novel strategy to restore natural antioxidant defenses in cardiovascular diseases.

Methods

Carotid artery injury model. Mice of various genetic backgrounds were anesthetized and subjected to left common carotid artery injury as previously described (3, 4) by topical application of a 1 × 2 mm piece of filter paper saturated with 7.5% or 12.5% $FeCl_3$ for 1 minute. Clot formation was observed in real time by fluorescence microscopy, and time to complete cessation of blood flow was determined through visual inspection using video image capture as previously described (3, 4). The end points of occlusion were set as (a) cessation of blood flow for more than 30 seconds and (b) no occlusion seen over the entire 30-minute time of observation (time was recorded as 30 minutes). In some studies, hydroethidine (10 μg/g in 150 μl saline) with or without edaravone (1 μg/g) was injected into the right jugular vein 5 minutes prior to carotid injury to detect ROS formation in the vessel wall. Fluorescence was recorded by intravital microscopy with a fixed exposure time of 2 ms throughout the observation period.

All procedures and manipulations of animals were approved by institutional animal care and use committees (IACUCs) at Cleveland Clinic in accordance with the United States Public Health Service Policy on the Humane Care and Use of Animals and the NIH *Guide for the care and use of laboratory animals* (8th edition. Revised 2010).

Immunohistochemical and immunofluorescence staining. After undergoing carotid artery thrombosis assays, mice were sacrificed and the thrombosed left carotid arteries were harvested, fixed in 4% formaldehyde overnight, and embedded in paraffin. Six-micrometer sections were cut, and immunohistochemical staining was performed for prdx2 expression. For frozen sections, the vessels were embedded in OCT and snap frozen in liquid nitrogen. For VSMC staining, cells were seeded in 4-well chamber glass slide (Lab-Tek), fixed in cold acetone (–20°C) for 10 minutes, washed with PBS, and permeabilized with 0.1% Triton X-100 in PBS for 5 minutes at room temperature. Slides were then incubated with primary antibodies followed by Alexa Fluor 488– or 594–conjugated secondary antibodies and then analyzed by laser confocal fluorescence microscopy using a Leica TCS-SP2 AOBS upright microscope. To quantify Nrf2 nuclear translocation, the fluorescence density of 15 randomly selected nuclei from 3 fields were analyzed by ImageJ software (NIH).

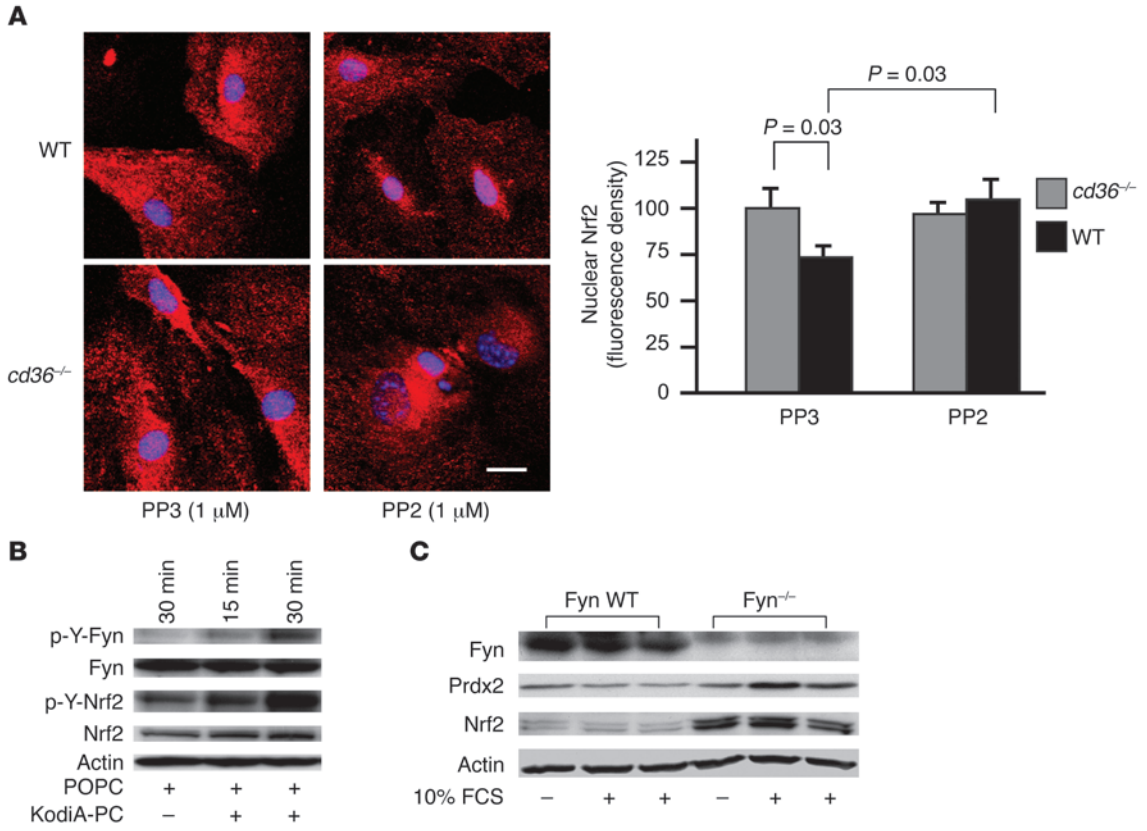

Figure 6

CD36-mediated Fyn activation promotes Nrf2 nuclear export and degradation. (**A**) Inhibition of src kinases increases accumulation of nuclear Nrf2. VSMCs were seeded in 4-well chambers on glass slides, synchronized, and then stimulated with complete medium in the presence of PP2 (1 μM) or PP3 (1 μM) for 60 minutes. Cells were then stained with anti-Nrf2 antibody and DAPI. 15 cells were randomly selected from 3 fields and nuclear Nrf2 density analyzed with NIH image. The lower panel shows cumulative data in a bar graph. The upper panel shows representative fields. Scale bar: 30 μm. One-way ANOVA (Bonferroni/Dunn) was used to determine the differences among groups. (**B**) CD36 ligand induces Fyn and Nrf2 tyrosine phosphorylation in VSMCs. VSMCs cultured as above were stimulated with POPC (final concentration 3.75 mM) vesicles containing KodiA-PC (final concentration 1.25 mM), a specific ligand of CD36, for indicated times. The cells were then lysed and immunoblots performed using antibody 4G10 to phosphotyrosine. The same membrane was stripped and reblotted with antibodies to Fyn, Nrf2, and actin. POPC vesicles without KodiA-PC were used as controls. (**C**) Fyn deletion increases Prdx2 and Nrf2 expression in VSMCs. VSMCs cultured from *fyn*$^{-/-}$ mice were stimulated with complete medium, and Fyn, Prdx2, and Nrf2 expression were examined by immunoblot. Actin was reblotted as loading control. Data are represented as mean ± SEM.

MP analysis. Heparin (100 USP in 100 μl saline) was injected into the right jugular vein prior to arterial injury to prevent thrombosis. After 1 minute application of $FeCl_3$, whole blood was collected 5 minutes later by cardiac puncture. 300 μl was diluted in 700 μl PBS, then centrifuged at 4300 *g* for 5 minutes to remove cells and large cell fragments. The supernatants were centrifuged at 100,000 *g* for 120 minutes at 4°C to pellet MPs. Pelleted MPs were resuspended in 50 μl HEPES-Tyrode's buffer and stored at –80°C (3). MP solutions (5 μl) were applied to siliconized glass slides and stained with FITC-conjugated anti–annexin V and anti-CD105 antibodies. Images were analyzed with laser confocal microscopy. MPs were also analyzed by a dot immunoblot assay using 10 μl of the MP solution and the same antibodies. Dot density was analyzed with NIH ImageJ.

Proteomic analysis of protein expression in carotid arteries. The uninjured right carotid arteries of 18 WT and 18 *cd36*$^{-/-}$ mice that had been subjected to $FeCl_3$-induced thrombosis in the contralateral carotid were harvested and pooled into 2 groups of 9; then proteins were extracted using the mirVana PARIS kit (Ambion). 100 μg from each extract was treated with the ReadyPrep 2-D Cleanup Kit (Bio-Rad). Proteins (50 μg) from WT mice were labeled with Cy3 (Invitrogen), those from *cd36*$^{-/-}$ mice with Cy5, and an internal control mixture from both mice (25 μg each) with Cy2. CyDye–labeled samples were mixed together, diluted to 450 μl with DeStreak Rehydration Solution (Amersham), and loaded onto a 24-cm IPG strip (pH 3-10 NL) gel for isoelectric focusing (IEF) using the Amersham IPGphor IEF system. The IPG strips were then reduced and alkylated and placed onto 24-cm Jule Pre-Cast Gels (12.5% SDS-PAGE) overlaid with 0.5% agarose in Laemmli buffer. Gels were run using an Ettan DALT 12 electrophoresis system. The 2D gels were scanned with the Typhoon imaging system and analyzed with DeCyder 6 software (GE). Gels were stained with Coomassie blue, and spots with more than 1.5-fold difference comparing WT and *cd36* nulls identified by DeCyder 6 analysis were picked and subjected to mass spectrometry analysis with LCQ or LTQ ion trap systems (Thermo Fisher).

Immunoblotting. Proteins (40 μg) from carotid extracts or cultured VSMCs were electrophoresed in 7.5% to 12.5% SDS-PAGE gradient gels

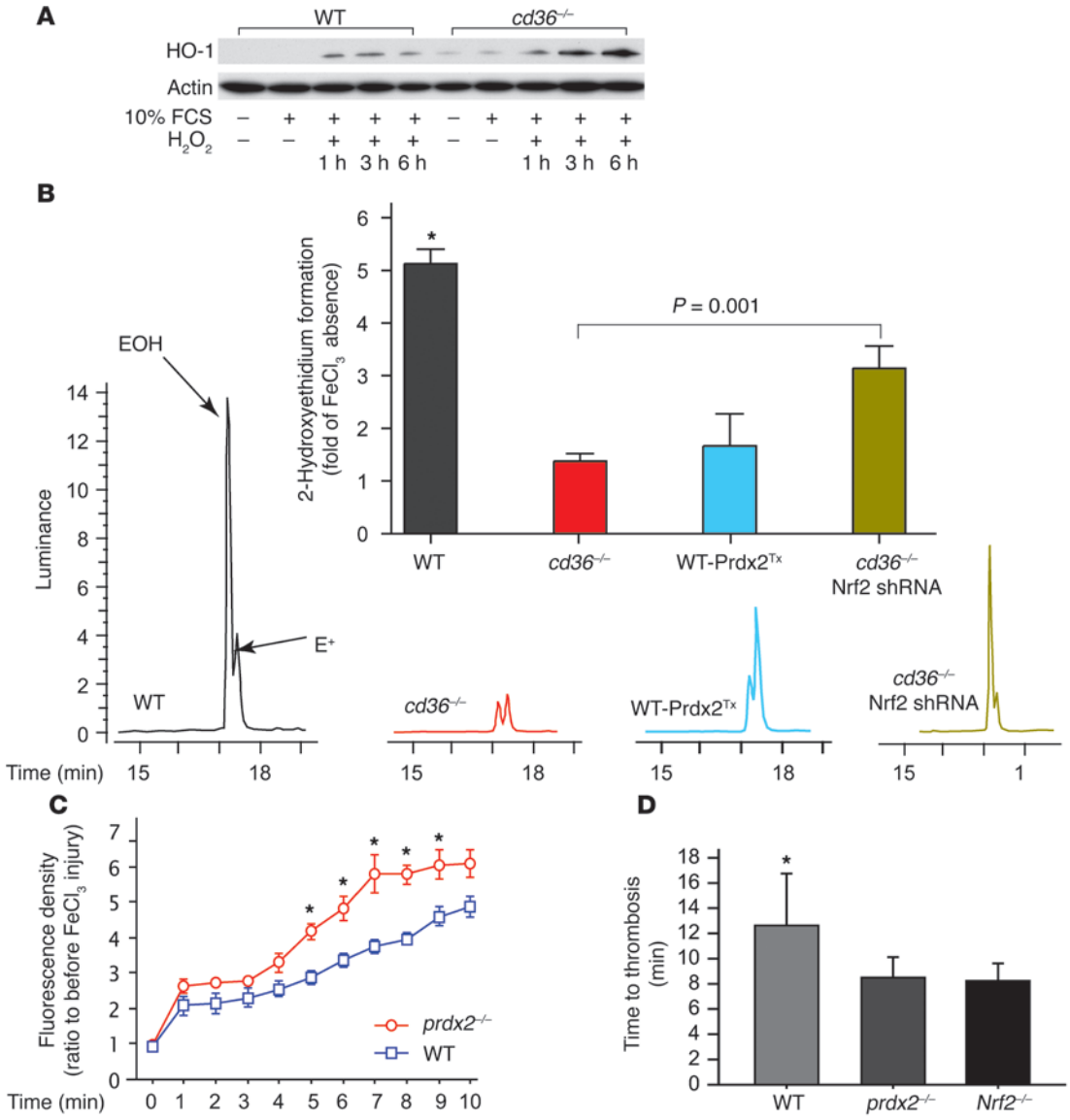

Figure 7

CD36 inhibits VSMC response to oxidative stress in vitro, and Prdx2 deficiency increases ROS generation and promotes thrombosis in vivo. (**A**) Western blot shows that *cd36*$^{-/-}$ cells have increased basal expression HO-1 compared with WT (lanes 6 and 7 versus lanes 1 and 2). After exposure to H_2O_2 (250 μM) for 3–6 hours, more HO-1 expression increased in the *cd36*$^{-/-}$ cells, but not in the WT. Stripped membranes were reblotted for actin as loading control. (**B**) Quantification of ROS in VSMCs by HPLC detection of EOH. WT, *cd36*$^{-/-}$, and human Prdx2 cDNA–transfected WT VSMCs or mouse Nrf2 shRNA–transfected *cd36*$^{-/-}$ VSMCs were treated with $FeCl_3$ for 30 minutes and incubated with DHE for another 30 minutes; cellular extracts were then examined by HPLC to detect and quantify EOH. Data are shown as fold changes of absence of $FeCl_3$ per se; $n = 3$. *$P < 0.001$ versus others. (**C**) Topical application of $FeCl_3$ induces increased ROS in carotid arteries of *prdx2*$^{-/-}$ mice. *prdx2*$^{-/-}$ and WT mice were treated as in Figure 1, and $FeCl_3$-induced ROS generation was detected using DHE as a fluorescence probe. *$P < 0.05$, *prdx2*$^{-/-}$ versus WT. (**D**) Prdx2 and Nrf2 deficiency are prothrombotic. Vessel occlusion time after $FeCl_3$-induced carotid artery injury was measured as in Figure 1 in *prdx2*$^{-/-}$, *nrf2*$^{-/-}$, and WT mice ($n = 8$ in each group). *$P < 0.01$, WT versus *prdx2*$^{-/-}$ or *nrf2*$^{-/-}$. One-way ANOVA (Bonferroni/Dunn) was used to determine the differences among groups. Data are represented as mean ± SEM.

and transferred onto PVDF membranes. After blockade with 5% nonfat milk, membranes were incubated with antibodies and developed with Amersham ECL Plus Western Blotting Detection Reagents. Membranes were stripped and reblotted with other antibodies. An anti-actin antibody was used as a loading control. The density of each band was analyzed with ATTO Densitography.

Primary VSMC culture. Mouse VSMC cultures were established from thoracic aorta explants of 8-week-old male mice as previously described (18, 49). Cells were identified as VSMCs by immunocytochemistry using a monoclonal antibody to smooth muscle α-actin (A2547; Sigma-Aldrich). Cell passages 4 to 12 were used in this study. After treatment, cells were washed with cold PBS and lysed in 20 mM MOPS, pH 7.0; 2 mM EGTA; 5 mM EDTA; 30 mM sodium fluoride; 60 mM β-glycerophosphate, pH 7.2; 20 mM sodium pyrophosphate; 1 mM sodium orthovanadate; 1% Triton X-100 containing proteinase inhibitor cocktail (Roche). BioVision Nuclear/Cytosol Fractionation Kit (BioVision

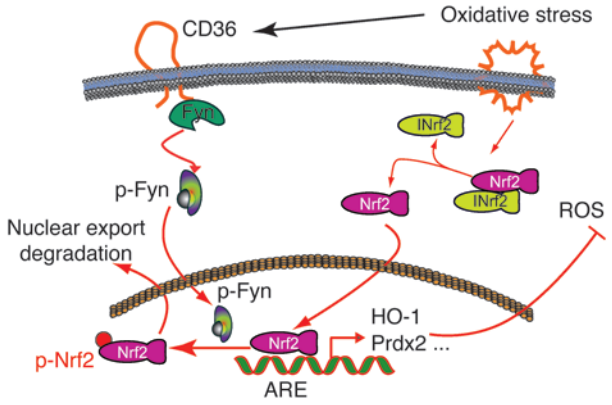

Figure 8
Model of CD36 regulation of ROS. Oxidative vascular injury leads to dissociation of the transcription factor Nrf2 from its cytoplasmic partner, Keap1/INrf2. Nrf2 then enters the nucleus, where it binds to specific ARE elements in key antioxidant genes, including HO-1 and Prdx2. Expression of these genes then attenuates oxidant stress. Oxidative stress also leads to generation of specific CD36 ligands, such as MP and oxLDL. Engagement of these ligands by CD36 recruits and activates Fyn kinase, which in turn phosphorylates Nrf2 in the nucleus. The phosphorylated Nrf2 is transported out of the nucleus and degraded.

Research Products) was used for extraction of cytosol and nuclear proteins based on the manufacturer's protocol.

NO_2LDL preparation, DiI labeling, and uptaking assay. LDL was isolated and purified from normal volunteers and was oxidized using a myeloperoxidase, glucose oxidase, nitrate system as previously described to generate NO_2LDL (50). NO_2LDL was labeled with the fluorescent probe DiI (Molecular Probes) as previously described (51). WT and *cd36*$^{-/-}$ VSMCs were seeded in 4-chamber slides at 10^3 cells/well, cultured for overnight, and then exposed to DiI-NO_2 LDL (10 μg/ml) for 60 minutes, fixed in 10% formalin, and analyzed by laser confocal microscopy.

ChIP assay. VSMCs were seeded at 2×10^6/10-cm plate, cultured overnight, and then synchronized for 24 hours prior to stimulation with DMEM containing 10% FCS for 3 hours. ChIP was performed using the EZchip Kit (Millipore) following the manufacturer's protocol. Anti-Nrf2 antibody (sc-722; Santa Cruz Biotechnology Inc.) and normal rabbit IgG were used to immunoprecipitate DNA/protein complexes. Two pairs of primers were designed to amplify the Prdx2 promoter region containing the cARE (forward: GACAGGTGACAGGTGCTTTCAGAT; reverse: TCAGCATCCTCATAGCACCTTAGA) and eARE (forward: CCTTCCTGATGCTGCGACCCTTTA; reverse: CCCCAGGATAGCAGCGAGCATTCA).

Luciferase assay. An 869-bp region from the Prdx2 promoter that includes the cARE, eARE, and eARE-like sites as well as truncated constructs from the same region shown in Supplemental Figure 1 and Figure 4B was amplified with specific primers. For mutation studies, the eARE site (TGAGGTAGCA) was divided into 3 parts as shown in Figure 4B and the nucleotides in each part were changed to thymine in the reverse primers. All of the forward primers were linked with AGCTTTACTCGAG at the 5′ end containing an *XhoI* recognition site, and reverse primers were linked with ACTGCAATAAGCTT at the 3′ end containing a *HindIII* recognition site. PCR products were cloned into a luciferase reporter vector, pGL2-Basic (Promega), and the plasmids then transformed into One Shot Top 10 competent cell (Invitrogen) and cultured and purified with QIAprep Spin Miniprep Kit (QIAGEN). 1 μg of each plasmid was transfected into WT VSMCs (cultured in 6-well) using Lipofectamine LTX and Plus Reagent (Invitrogen). Luciferase reporter activities were examined 48 hours later using an assay kit from Promega.

Real-time PCR–based mRNA quantitation assay. Total RNA was extracted from VSMCs using RNeasy Mini Kit (QIAGEN). 1 μg of the total RNA was treated with DNase I, and cDNA was constructed using AMV First Strand cDNA Synthesis Kit for RT-PCR (Roche). Real-time PCR was performed using SYBR Green PCR Master Mix (Applied Biosystems) with an iCycler iQ Real-Time PCR detection system (52).

Plasmids and transfections. The pCDNA3/mNrf2 plasmid vector (53), empty pCDNA3 vector, and pCR3.1/hPrdx2 plasmid (54) were transfected into WT VSMCs using the Lipofectamine LTX and Plus Reagent, and cells were selected with G418 antibiotic. A pool of Nrf2- or Prdx2-overexpressing cells as well as pcDNA empty vector control cells was established and expressions of Nrf2 as well as Prdx2 were examined by Western blot. In other experiments, mouse Nrf2 shRNA plasmid (Santa Cruz Biotechnology Inc.) was transfected into *cd36*$^{-/-}$ cells as above and a cell pool was selected with puromycin (7.5 μg/ml final concentration). Prdx2 expression after *nrf2* gene knockdown in *cd36*$^{-/-}$ cells was examined by Western blot assay.

HPLC-based superoxide quantification. 2×10^6 VSMCs were seeded on 10-cm plates and cultured for 24 hours. The cells were then treated with $FeCl_3$ in a final concentration of 0.05% to 0.2% in culture media for 30 minutes at 37°C (27) and then washed with cold PBS 2 times and incubated in 3 ml Hanks' buffer composed of 1.3 mM $CaCl_2$, 0.8 mM $MgSO_4$, 5.4 mM KCl, 0.4 mM KH_2PO_4, 4.3 mM $NaHCO_3$, 137 mM NaCl, 0.3 mM Na_2HPO_4, and 5.6 mM glucose, pH 7.4, containing diethylenetriamine pentaacetic acid (DTPA) (100 μM) and a final DHE concentration of 50 μM for an additional 30 minutes at 37°C. Cells were washed twice with cold PBS, harvested in acetonitrile (1.5 ml/plate), sonicated (10 s, 1 cycle at 8 w), and centrifuged at 12,000 *g* for 10 minutes at 4°C (25). Supernatants were lyophilized to dryness and pellets maintained at –20°C in the dark until analyzed. Samples were resuspended in 150 μl PBS/DTPA (100 μM) and 100 μl aliquots injected into a 250 mm × 4.6 mm, 5 μm Kromasil C18 column on an HPLC system (Agilent 1100; Agilent Technologies). Solutions A (pure acetonitrile) and B (water/10% acetonitrile/0.1% trifluoroacetic acid) were used as a mobile phase at a flow rate of 0.5 ml/min (25). DHE was monitored by ultraviolet absorption at 245 nm. EOH and ethidium were monitored by fluorescence detection with excitation 510 nm and emission 595 nm. Quantification was performed by comparison of integrated peak areas between the obtained and standard solutions under identical chromatographic conditions. EOH standard was prepared as previously described (15).

Statistics. One-way ANOVA (Bonferroni/Dunn) was used to determine the differences among groups. Unpaired *t* test was used to determine differences between groups. Data were represented as mean ± SEM, and $P < 0.05$ was considered significant. Each in vitro experiment was repeated as least 3 times with different passage cells.

Acknowledgments

This project was supported by NIH grants HL81011 and HL092747 (to R.L. Silverstein) and HL66109 (to S.P. Reddy). We thank Patricia DiBello in the Cleveland Clinic Department of Cell Biology for her assistance in HPLC analysis.

Received for publication March 1, 2010, and accepted in revised form August 25, 2010.

Address correspondence to: Roy L. Silverstein, Department of Cell Biology/NC10, Lerner Research Institute, Cleveland Clinic Foundation, 9500 Euclid Ave., Cleveland, Ohio 44195, USA. Phone: 216.444.5220; Fax: 216.444.9404; E-mail: silverr2@ccf.org.

1. Silverstein RL, Febbraio M. CD36, a scavenger receptor involved in immunity, metabolism, angiogenesis, and behavior. *Sci Signal*. 2009;2(72):re3.
2. Podrez EA, et al. Platelet CD36 links hyperlipidemia, oxidant stress and a prothrombotic phenotype. *Nat Med*. 2007;13(9):1086–1095.
3. Ghosh A, et al. Platelet CD36 mediates interactions with endothelial cell-derived microparticles and contributes to thrombosis in mice. *J Clin Invest*. 2008;118(5):1934–1943.
4. Chen K, Febbraio M, Li W, Silverstein RL. A specific CD36-dependent signaling pathway is required for platelet activation by oxidized low-density lipoprotein. *Circ Res*. 2008;102(12):1512–1519.
5. Swerlick RA, Lee KH, Wick TM, Lawley TJ. Human dermal microvascular endothelial but not human umbilical vein endothelial cells express CD36 in vivo and in vitro. *J Immunol*. 1992;148(1):78–83.
6. Dawson DW, et al. CD36 mediates the In vitro inhibitory effects of thrombospondin-1 on endothelial cells. *J Cell Biol*. 1997;138(3):707–717.
7. Matsumoto K, et al. Expression of macrophage (Mphi) scavenger receptor, CD36, in cultured human aortic smooth muscle cells in association with expression of peroxisome proliferator activated receptor-gamma, which regulates gain of Mphi-like phenotype in vitro, and its implication in atherogenesis. *Arterioscler Thromb Vasc Biol*. 2000; 20(4):1027–1032.
8. Ricciarelli R, Zingg JM, Azzi A. Vitamin E reduces the uptake of oxidized LDL by inhibiting CD36 scavenger receptor expression in cultured aortic smooth muscle cells. *Circulation*. 2000;102(1):82–87.
9. Lim HJ, et al. PPARgamma activation induces CD36 expression and stimulates foam cell like changes in rVSMCs. *Prostaglandins Other Lipid Mediat*. 2006; 80(3–4):165–174.
10. Kwok CF, Juan CC, Ho LT. Endothelin-1 decreases CD36 protein expression in vascular smooth muscle cells. *Am J Physiol Endocrinol Metab*. 2007; 292(2):E648–E652.
11. de Oliveira Silva C, Delbosc S, Araïs C, Monnier L, Cristol JP, Pares-Herbute N. Modulation of CD36 protein expression by AGEs and insulin in aortic VSMCs from diabetic and non-diabetic rats. *Nutr Metab Cardiovasc Dis*. 2008;18(1):23–30.
12. Xue JH, et al. High glucose promotes intracellular lipid accumulation in vascular smooth muscle cells by impairing cholesterol influx and efflux balance. *Cardiovasc Res*. 2009;86(1):141–150.
13. Cho S, et al. The class B scavenger receptor CD36 mediates free radical production and tissue injury in cerebral ischemia. *J Neurosci*. 2005;25(10):2504–2512.
14. Cho S, Szeto HH, Kim E, Kim H, Tolhurst AT, Pinto JT. A novel cell-permeable antioxidant peptide, SS31, attenuates ischemic brain injury by down-regulating CD36. *J Biol Chem*. 2007;282(7):4634–4642.
15. Zhao H, et al. Superoxide reacts with hydroethidine but forms a fluorescent product that is distinctly different from ethidium: potential implications in intracellular fluorescence detection of superoxide. *Free Radic Biol Med*. 2003;34(11):1359–1368.
16. Low FM, Hampton MB, Peskin AV, Winterbourn CC. Peroxiredoxin 2 functions as a noncatalytic scavenger of low-level hydrogen peroxide in the erythrocyte. *Blood*. 2007;109(6):2611–2617.
17. Low FM, Hampton MB, Winterbourn CC. Peroxiredoxin 2 and peroxide metabolism in the erythrocyte. *Antioxid Redox Signal*. 2008;10(9):1621–1630.
18. Li W, et al. Thymidine phosphorylase gene transfer inhibits vascular smooth muscle cell proliferation by upregulating heme oxygenase-1 and p27KIP1. *Arterioscler Thromb Vasc Biol*. 2005;25(7):1370–1375.
19. Lee JM, et al. Nrf2, a multi-organ protector? *FASEB J*. 2005;19(9):1061–1066.
20. Nerland DE. The antioxidant/electrophile response element motif. *Drug Metab Rev*. 2007;39(1):235–248.
21. Nioi P, McMahon M, Itoh K, Yamamoto M, Hayes JD. Identification of a novel Nrf2-regulated antioxidant response element (ARE) in the mouse NAD(P)H:quinone oxidoreductase 1 gene: reassessment of the ARE consensus sequence. *Biochem J*. 2003;374(pt 2):337–348.
22. Huang MM, Bolen JB, Barnwell JW, Shattil SJ, Brugge JS. Membrane glycoprotein IV (CD36) is physically associated with the Fyn, Lyn, and Yes protein-tyrosine kinases in human platelets. *Proc Natl Acad Sci U S A*. 1991;88(17):7844–7848.
23. Jain AK, Jaiswal AK. Phosphorylation of tyrosine 568 controls nuclear export of Nrf2. *J Biol Chem*. 2006;281(17):12132–12142.
24. Podrez EA, et al. Identification of a novel family of oxidized phospholipids that serve as ligands for the macrophage scavenger receptor CD36. *J Biol Chem*. 2002;277(41):38503–38516.
25. Fernandes DC, et al. Analysis of DHE-derived oxidation products by HPLC in the assessment of superoxide production and NADPH oxidase activity in vascular systems. *Am J Physiol Cell Physiol*. 2007;292(1):C413–C422.
26. Zielonka J, Vasquez-Vivar J, Kalyanaraman B. Detection of 2-hydroxyethidium in cellular systems: a unique marker product of superoxide and hydroethidine. *Nat Protoc*. 2008;3(1):8–21.
27. Willmore LJ, Hiramatsu M, Kochi H, Mori A. Formation of superoxide radicals after FeCl3 injection into rat isocortex. *Brain Res*. 1983;277(2):393–396.
28. Fearon IM, Faux SP. Oxidative stress and cardiovascular disease: novel tools give (free) radical insight. *J Mol Cell Cardiol*. 2009;47(3):372–381.
29. Steinberg D. Atherogenesis in perspective: hypercholesterolemia and inflammation as partners in crime. *Nat Med*. 2002;8(11):1211–1217.
30. Blum A. The possible role of red blood cell microvesicles in atherosclerosis. *Eur J Intern Med*. 2009;20(2):101–105.
31. Collot-Teixeira S, Martin J, McDermott-Roe C, Poston R, McGregor JL. CD36 and macrophages in atherosclerosis. *Cardiovasc Res*. 2007;75(3):468–477.
32. Febbraio M, Hajjar DP, Silverstein RL. CD36: a class B scavenger receptor involved in angiogenesis, atherosclerosis, inflammation, and lipid metabolism. *J Clin Invest*. 2001;108(6):785–791.
33. Febbraio M, et al. Targeted disruption of the class B scavenger receptor CD36 protects against atherosclerotic lesion development in mice. *J Clin Invest*. 2000;105(8):1049–1056.
34. Rahaman SO, Lennon DJ, Febbraio M, Podrez EA, Hazen SL, Silverstein RL. A CD36-dependent signaling cascade is necessary for macrophage foam cell formation. *Cell Metab*. 2006;4(3):211–221.
35. Park YM, Febbraio M, Silverstein RL. CD36 modulates migration of mouse and human macrophages in response to oxidized LDL and may contribute to macrophage trapping in the arterial intima. *J Clin Invest*. 2009;119(1):136–145.
36. Knowles JW, et al. Association of polymorphisms in platelet and hemostasis system genes with acute myocardial infarction. *Am Heart J*. 2007;154(6):1052–1058.
37. Pellikka M, Narhi L, Perola M, Penttila A, Karhunen PJ, Mikkelsson J. Platelet GPIbalpha, GPIV and vWF polymorphisms and fatal pre-hospital MI among middle-aged men. *J Thromb Thrombolysis*. 2008;26(2):91–96.
38. Kennedy DJ, et al. Dietary cholesterol plays a role in CD36-mediated atherogenesis in LDLR-knockout mice. *Arterioscler Thromb Vasc Biol*. 2009; 29(10):1481–1487.
39. Sukhanov S, et al. Novel effect of oxidized low-density lipoprotein: cellular ATP depletion via downregulation of glyceraldehyde-3-phosphate dehydrogenase. *Circ Res*. 2006;99(2):191–200.
40. Ishii T, et al. Role of Nrf2 in the regulation of CD36 and stress protein expression in murine macrophages: activation by oxidatively modified LDL and 4-hydroxynonenal. *Circ Res*. 2004;94(5):609–616.
41. Hernandez-Trujillo Y, Rodriguez-Esparragon F, Macias-Reyes A, Caballero-Hidalgo A, Rodriguez-Perez JC. Rosiglitazone but not losartan prevents Nrf–2 dependent CD36 gene expression up–regulation in an in vivo atherosclerosis model. *Cardiovasc Diabetol*. 2008;7:3.
42. D'Archivio M, et al. Oxidised LDL up-regulate CD36 expression by the Nrf2 pathway in 3T3-L1 preadipocytes. *FEBS Lett*. 2008;582(15):2291–2298.
43. Maruyama A, et al. Nrf2 regulates the alternative first exons of CD36 in macrophages through specific antioxidant response elements. *Arch Biochem Biophys*. 2008;477(1):139–145.
44. Sussan TE, et al. Disruption of Nrf2, a key inducer of antioxidant defenses, attenuates ApoE-mediated atherosclerosis in mice. *PLoS One*. 2008; 3(11):e3791.
45. Inkala M, et al. Nrf2 expression in macrophages does not promote atherosclerosis in hyperlipidemic mouse model of atherosclerosis. Abstract 174. Poster presented at: Council on Arteriosclerosis, Thrombosis and Vascular Biology, 2010; April 8–10, 2010; San Francisco, California, USA.
46. Li J, et al. Nrf2 protects against maladaptive cardiac responses to hemodynamic stress. *Arterioscler Thromb Vasc Biol*. 2009;29(11):1843–1850.
47. Levonen AL, et al. Nrf2 gene transfer induces antioxidant enzymes and suppresses smooth muscle cell growth in vitro and reduces oxidative stress in rabbit aorta in vivo. *Arterioscler Thromb Vasc Biol*. 2007;27(4):741–747.
48. Juan SH, et al. Adenovirus-mediated heme oxygenase-1 gene transfer inhibits the development of atherosclerosis in apolipoprotein E-deficient mice. *Circulation*. 2001;104(13):1519–1525.
49. Yue H, Lee JD, Shimizu H, Uzui H, Mitsuke Y, Ueda T. Effects of magnesium on the production of extracellular matrix metalloproteinases in cultured rat vascular smooth muscle cells. *Atherosclerosis*. 2003;166(2):271–277.
50. Podrez EA, Schmitt D, Hoff HF, Hazen SL. Myeloperoxidase-generated reactive nitrogen species convert LDL into an atherogenic form in vitro. *J Clin Invest*. 1999;103(11):1547–1560.
51. Pitas RE, Innerarity TL, Weinstein JN, Mahley RW. Acetoacetylated lipoproteins used to distinguish fibroblasts from macrophages in vitro by fluorescence microscopy. *Arteriosclerosis*. 1981;1(3):177–185.
52. Li W, et al. Role of MMPs and plasminogen activators in angiogenesis after transmyocardial laser revascularization in dogs. *Am J Physiol Heart Circ Physiol*. 2003;284(1):H23–H30.
53. Katoh Y, Itoh K, Yoshida E, Miyagishi M, Fukamizu A, Yamamoto M. Two domains of Nrf2 cooperatively bind CBP, a CREB binding protein, and synergistically activate transcription. *Genes Cells*. 2001;6(10):857–868.
54. Kang SW, Chae HZ, Seo MS, Kim K, Baines IC, Rhee SG. Mammalian peroxiredoxin isoforms can reduce hydrogen peroxide generated in response to growth factors and tumor necrosis factor-alpha. *J Biol Chem*. 1998;273(11):6297–6302.